J|A|C|S
ARTICLES
Published on Web 06/02/2005

Direct Tyrosine Oxidation Using the MLCT Excited States of Rhenium Polypyridyl Complexes

Steven Y. Reece and Daniel G. Nocera*

Contribution from the Department of Chemistry, 6-335, Massachusetts Institute of Technology, 77 Massachusetts Avenue, Cambridge, Massachusetts 02139-4307

Received February 17, 2005; E-mail: nocera@mit.edu

Abstract: Rhenium(I) polypyridyl complexes have been designed for the intramolecular photogeneration of tyrosyl radical. Tyrosine (Y) and phenylalanine (F) have each been separately appended to a conventional $Re^{I}(bpy)(CO)_3CN$ framework via an amide linkage to the bipyridine (bpy) ligand. Comparative time-resolved emission quenching and transient absorption spectra of $Re(bpy\text{-}Y)(CO)_3CN$ and $Re(bpy\text{-}F)(CO)_3CN$ show that Y is oxidized only upon its deprotonation at pH 12. In an effort to redirect electron transport so that it is more compatible with intramolecular Y oxidation, polypyridyl Re^{I} complexes have been prepared with the amide bond functionality located on a pendant phosphine ligand. A $[Re(phen)(PP\text{-}Bn)(CO)_2](PF_6)$ (PP = bis(diphenylphosphino)ethylene) complex has been synthesized and crystallographically characterized. Electrochemistry and phosphorescence measurements of this complex indicate a modest excited-state potential for tyrosine oxidation, similar to that for the $(bpy)Re^{I}(CO)_3CN$ framework. The excited-state oxidation potential can be increased by introducing a monodentate phosphine to the $Re^{I}(NN)(CO)_3^{+}$ framework (NN = polypyridyl). In this case, Y is oxidized at all pHs when appended to the triphenylphosphine (P) of $[Re(phen)(P\text{-}Y)(CO_3)](PF_6)$. Analysis of the pH dependence of the rate constant for tyrosyl radical generation is consistent with a proton-coupled electron transfer (PCET) quenching mechanism.

Introduction

Amino acid radicals are increasingly identified as reactive intermediates along the primary metabolic pathways of many enzymes.[1] Owing to their high reactivity, the radicals are often present as fleeting intermediates along a directed pathway so as to minimize their time for participation in deleterious one-electron/radical side reactions. Accordingly, investigations of reaction mechanisms involving amino acid radicals require methods to generate the radical on fast time scales. Of the various time-resolved methods available, laser flash photolysis techniques provide the largest temporal window for mechanistic studies because reactions may be turned on "instantaneously" with a pulse of light. Nowhere are the benefits of this approach better exemplified than in the study of electron transfer (ET) in biology. First developed for the ET reactions of modified cytochromes[2,3] and subsequently generalized to other proteins and enzymes,[4−13] the laser flash photolysis approach can initiate the reaction on a time scale fast enough to allow for direct observation of the actual ET tunneling event. The same temporal benefits may be retained for mechanistic investigations of amino acid radicals with the caveat that both electron and proton inventories need to be managed[14,15] in the generation of the amino acid radical. The photon energy must, therefore, be sufficiently energetic to overcome barriers for both electron and proton transfer.[16−21] We have been particularly interested in photogenerating tyrosyl radical ($Y^{\bullet}$) and modified derivatives for the study of the 35 Å proton-coupled electron transfer (PCET) pathway of class I ribonucleotide reductases (RNRs).[22−25] Methods have been developed to photogenerate $Y^{\bullet}$ by laser

(1) Stubbe, J.; van der Donk, W. A. *Chem. Rev.* **1998**, *98*, 705.
(2) Winkler, J. R.; Nocera, D. G.; Yocom, K. M.; Bordignon, E.; Gray, H. B. *J. Am. Chem. Soc.* **1982**, *104*, 5798.
(3) Nocera, D. G.; Winkler, J. R.; Yocom, K. M.; Bordignon, E.; Gray, H. B. *J. Am. Chem. Soc.* **1984**, *106*, 5145.
(4) *Electron Transfer in Chemistry*; Balzani, V., Ed.; Wiley-VCH: Weinheim, Germany, 2001; Vol. 3, Part 1.
(5) Gray, H. B.; Winkler, J. R. *Annu. Rev. Biochem.* **1996**, *65*, 537.
(6) Farver, O.; Pecht, I. *Biophys. Chem.* **1994**, *50*, 203.
(7) Davidson, V. L. *Acc. Chem. Res.* **2000**, *33*, 87.
(8) McLendon, G.; Hake, R. *Chem. Rev.* **1992**, *92*, 481.
(9) Gunner, M. R.; Robertson, D. E.; Dutton, P. L. *J. Phys. Chem.* **1986**, *90*, 3783.
(10) Namslauer, A.; Braenden, M.; Brzezinski, P. *Biochemistry* **2002**, *41*, 10369.
(11) Millett, F. S. *J. Bioenerg. Biomembr.* **1995**, *27*, 261.
(12) Wang, K.; Zhen, Y.; Sadoski, R.; Grinnell, S.; Geren, L.; Ferguson-Miller, S.; Durham, B.; Millett, F. *J. Biol. Chem.* **1999**, *274*, 38042.
(13) Nocek, J. M.; Zhou, J. S.; Forest, S. D.; Priyadarshy, S.; Beratan, D. N.; Onuchic, J. N.; Hoffman, B. M. *Chem. Rev.* **1996**, *96*, 2459.
(14) Cukier, R. I.; Nocera, D. G. *Annu. Rev. Phys. Chem.* **1998**, *49*, 337.
(15) Chang, C. J.; Chang, M. C. Y.; Damrauer, N. H.; Nocera, D. G. *Biochim. Biophys. Acta* **2004**, *1655*, 13.
(16) Damrauer, N. H.; Hodgkiss, J. M.; Rosenthal, J.; Nocera, D. G. *J. Phys. Chem. B* **2004**, *108*, 6315.
(17) Kirby, J. P.; Roberts, J. A.; Nocera, D. G. *J. Am. Chem. Soc.* **1997**, *119*, 9230.
(18) Roberts, J. A.; Kirby, J. P.; Nocera, D. G. *J. Am. Chem. Soc.* **1995**, *117*, 8051.
(19) Deng, Y.; Roberts, J. A.; Peng, S.-M.; Chang, C. K.; Nocera, D. G. *Angew. Chem., Int. Ed. Engl.* **1997**, *36*, 2124.
(20) Roberts, J. A.; Kirby, J. P.; Wall, S. T.; Nocera, D. G. *Inorg. Chim. Acta* **1997**, *263*, 395.
(21) Turró, C.; Chang, C. K.; Leroi, G. E.; Cukier, R. I.; Nocera, D. G. *J. Am. Chem. Soc.* **1992**, *114*, 4013.
(22) Stubbe, J.; Nocera, D. G.; Yee, C. S.; Chang, M. C. Y. *Chem. Rev.* **2003**, *103*, 2167.
(23) Yee, C. S.; Chang, M. C. Y.; Ge, J.; Nocera, D. G.; Stubbe, J. *J. Am. Chem. Soc.* **2003**, *125*, 10506.
(24) Yee, C. S.; Seyedsayamdost, M. R.; Chang, M. C. Y.; Nocera, D. G.; Stubbe, J. *Biochemistry* **2003**, *42*, 14541.
(25) Chang, M. C. Y.; Yee, C. S.; Nocera, D. G.; Stubbe, J. *J. Am. Chem. Soc.* **2004**, *126*, 16702.

10.1021/ja0510360 CCC: $30.25

excitation of tyrosine oxalate esters[26] and through photoionization of tryptophan (W), producing W$^{\bullet}$ which in turn oxidizes Y below pH 10.[27] In both cases, a UV exciting photon is needed to overcome the barriers for radical generation. Whereas the intrinsic efficiency for Y$^{\bullet}$ photogeneration is high, radical yields are mitigated in the biological milieu owing to high absorption cross-sections of UV photons by proteins.[28] We, therefore, have sought new photochemical methods for Y$^{\bullet}$ generation in higher yields using an excitation profile to the red of protein absorption envelopes.

Metal-to-ligand charge transfer (MLCT) excited states of metal complexes can be used to initiate biological redox processes using visible light. The MLCT excited state of Ru^{II} bipyridyl (bpy) and its derivatives has been especially useful for redox processes involving metallo-cofactors.[4] Owing to the modest redox potential of Ru^{II} polypyridyl MLCT excited states, their application is best-suited for the study of ET reactions involving metal-containing cofactors with mild reduction potentials, such as hemes,[3] iron−sulfur clusters,[29] and blue copper proteins.[30] The utility of the Ru^{II} polypyridyl MLCT excited state may be extended when implemented as part of the flash-quench method.[31,32] With this technique, the more powerfully reducing Ru^{I} or oxidizing Ru^{III} centers are photogenerated by bimolecularly quenching the MLCT excited state with an external reductant or oxidant, respectively. The Ru^{I} or Ru^{III} complex persists with sufficient lifetime, owing to a slow bimolecular back-reaction or irreversible quenching step, to enable it to initiate a subsequent redox process on time scales longer than that for the decay of the corresponding MLCT excited state. Owing to the greater oxidizing and reducing power of the flash-quenched products, as compared to that of the Ru^{II} MLCT excited state, redox processes of nonmetal-based cofactors may be initiated. The approach has been extended to amino acid radicals by Hammarström and co-workers,[33] who using the flash-quench-generated Ru^{III}(bpy)$_3^{3+}$, observed oxidation of a tyrosine residue covalently bound to one of the bpy ligands. The rate of charge transport is 5×10^4 s^{-1}, and tyrosyl radical formation occurs by a PCET mechanism with proton loss to bulk solvent.[34,35] The rate for radical generation can be accelerated by increasing the oxidizing strength of the flash-quenched product. For instance, a Re(NN)(CO)$_3$(Q107H)$^+$-modified azurin Y108W mutant can be flash-quenched to generate the Re^{II} oxidation state, which in turn has been observed to oxidize the adjacent W108 residue to •W108 with a rate constant of 2.8×10^6 s^{-1}.[36,37] Flash quench of the same complex in the protein with the native Y108 residue appears to produce •Y108; however, the reaction was not kinetically characterized.[38]

The implementation of the flash-quench method becomes more cumbersome when the electron and proton transfer events are coupled to the chemistry of a functioning enzyme. This is the case for the radical chemistry in RNR, where typical quenchers of the flash-quench method can directly interfere with allosteric regulation of the enzyme, radical intermediates of the PCET pathway, and the chemistry attendant to substrate activation and turnover. For these reasons, we are interested in developing more reactive photo-oxidants that can efficiently produce tyrosine radicals directly from an MLCT excited state without the need for external quenchers. We now describe the synthesis of Re^{I} polypyridyl complexes with primary coordination spheres that are covalently modified with tyrosine along with the kinetics and mechanism for the photogeneration of tyrosyl radical directly from the MLCT excited state.

Experimental Section

Materials and Methods. L-Tyrosine *tert*-butyl ester (Y-O*t*Bu), L-alanine *tert*-butyl ester hydrochloride (A-O*t*Bu•HCl), 1-hydroxybenzotriazole (HOBt) (NovaBiochem), L-phenylalanine *tert*-butyl ester hydrochloride (F−O*t*Bu•HCl) (Advanced ChemTech), magnesium sulfate ($MgSO_4$) (EMD), thallium hexafluorophosphate ($TlPF_6$) (Strem), potassium thiocyanate (KSCN), sodium cyanide (NaCN), 1-(3-(dimethylamino)propyl)-3-ethylcarbodiimide hydrochloride (WSC•HCl), 4-(dimethylamino)pyridine (DMAP), *N*-methylmorpholine (NMM), pentacarbonylchlororhenium ($Re(CO)_5Cl$), 1,10-phenanthroline (phen), 4-diphenylphosphinobenzoic acid (Ph_2PPh−COOH) (Aldrich), and trifluoroacetic acid (TFA, 99.9%) (J. T. Baker) were used as received. 4′-Methyl-2,2′-bipyridine-4-carboxylic acid (bpy−COOH),[39] *cis*-1,2-(bisdiphenylphospino)ethylene-(1,10-phenanthroline)(dicarbonyl)rhenium(I) hexafluorophosphate ($[Re(phen)(dppe)(CO)_2](PF_6)$),[40] and tricarbonylchloro(1,10-phenanthroline)rhenium(I) ($Re(phen)(CO)_3Cl$)[41] were prepared as previously described. *cis*-1-Carboxy-2-(*N*-benzylcarbamoyl)-1,2-bis(diphenylphosphino)ethene (HOOC-PP-Bn)[42] was prepared from 2,3-bis(diphenylphosphino)maleic anhydride (bma)[43] and benzylamine (Aldrich).

Tricarbonylchloro(4′-methyl-2,2′-bipyridine-4-carboxylic acid)-rhenium(I) (Re(bpy−COOH)(CO)$_3$Cl). $Re(CO)_5Cl$ (347 mg, 0.962 mmol, 1.0 equiv) and bpy-COOH (206 mg, 0.962 mmol, 1.0 equiv) were added to toluene (25 mL) contained in a round-bottom flask, and the mixture was heated at reflux overnight. The bright orange solution was cooled to room temperature, and the yellow/orange solid was isolated by filtration, washed with ether, and dried under vacuum (470 mg, 94%). ^{1}H NMR (300 MHz, d-acetone, 25 °C): $\delta = 2.67$ (s, 3H, bpy-CH_3), 7.66 (m, 1H, bpy-H), 8.21 (m, 1H, bpy-H), 8.81 (s, 1H, bpy-H), 8.95 (d, 1H, bpy-H), 9.00 (s, 1H, bpy-H), 9.29 (d, 1H, bpy-H). ^{1}H NMR (300 MHz, CD_3OD, 25 °C): $\delta = 2.62$ (s, 3H, bpy-CH_3), 7.55 (m, 1H, bpy-H), 8.13 (m, 1H, bpy-H), 8.57 (s, 1H, bpy-H), 8.87 (d, 1H, bpy-H), 8.98 (s, 1H, bpy-H), 9.19 (d, 1H, bpy-H).

(26) Chang, M. C. Y.; Miller, S. E.; Carpenter, S. D.; Stubbe, J.; Nocera, D. G. *J. Org. Chem.* **2002**, *67*, 6820.
(27) Reece, S. Y.; Stubbe, J.; Nocera, D. G. *Biophys. Biochim. Acta* **2005**, *1706*, 232.
(28) Chang, M. C. Y.; Yee, C. S.; Stubbe, J.; Nocera, D. G. *Proc. Natl. Acad. Sci. U.S.A.* **2004**, *101*, 6882.
(29) Babini, E.; Bertini, I.; Borsari, M.; Capozzi, F.; Luchinat, C.; Zhang, X.; Moura, G. L. C., IV; Kurnikov, D. N.; Beratan, A.; Ponce, A.; Di Bilio, A. J.; Winkler, J. R.; Gray, H. B. *J. Am. Chem. Soc.* **2000**, *122*, 4532.
(30) Pascher, T.; Karlsson, B. G.; Nordling, M.; Malmström, B. G.; Vanngård, T. *Eur. J. Biochem.* **1993**, *212*, 289.
(31) Chang, I.-J.; Gray, H. B.; Winkler, J. R. *J. Am. Chem. Soc.* **1991**, *113*, 7056.
(32) Bjerrum, M. J.; Casimiro, D. R.; Chang, I. J.; Di Bilio, A. J.; Gray, H. B.; Hill, M. G.; Langen, R.; Mines, G. A.; Skov, L. K.; Winkler, J. R. *J. Bioenerg. Biomembr.* **1995**, *27*, 295.
(33) Magnuson, A.; Berglund, P.; Korral, P.; Hammarström, L.; Åkermark, B.; Styring, S.; Sun, L. C. *J. Am. Chem. Soc.* **1997**, *119*, 10720.
(34) Sjödin, M.; Styring, S.; Åkermark, B.; Sun, L.; Hammarström, L. *J. Am. Chem. Soc.* **2000**, *122*, 3932.
(35) Sjödin, M.; Styring, S.; Wolpher, H.; Xu, Y.; Sun, L.; Hammarström, L. *J. Am. Chem. Soc.* **2005**, *127*, 3855.
(36) Miller, J. E.; Grãdinaru, C.; Crane, B. R.; Di Bilio, A. J.; Wehbi, W. A.; Un, S.; Winkler, J. R.; Gray, H. B. *J. Am. Chem. Soc.* **2003**, *125*, 14220.
(37) Miller, J. E.; DiBilio, A. J.; Wehbi, W. A.; Green, M. T.; Museth, A. K.; Richards, J. R.; Winkler, J. R.; Gray, H. B. *Biochim. Biophys. Acta* **2004**, *1655*, 59.
(38) Di Bilio, A. J.; Crane, B. R.; Wehbi, W. A.; Kiser, C. N.; Abu-Omar, M. M.; Carlos, R. M.; Richards, J. H.; Winkler, J. R.; Gray, H. B. *J. Am. Chem. Soc.* **2001**, *123*, 3181.
(39) McCafferty, D. G.; Bishop, B. M.; Wall, C. G.; Hughes, S. G.; Mecklenberg, S. L.; Meyer, T. J.; Erickson, B. W. *Tetrahedron* **1995**, *51*, 1093.
(40) Schutte, E.; Helms, J. B.; Woessner, S. M.; Bowen, J.; Sullivan, B. P. *Inorg. Chem.* **1998**, *37*, 2618.
(41) Wrighton, M.; Morse, D. L. *J. Am. Chem. Soc.* **1974**, *96*, 998.
(42) Lewis, J. S.; Heath, S. L.; Powell, A. K.; Zweit, J.; Blower, P. J. *J. Chem. Soc., Dalton Trans.* **1997**, *5*, 855.
(43) Mao, F.; Sur, S. K.; Tyler, D. R. *Organometallics* **1991**, *10*, 419.

Tricarbonylthiocyanato(4′-methyl-2,2′-bipyridine-4-carboxylic acid)rhenium(I) (Re(bpy-COOH)(CO)$_3$SCN). Re(bpy-COOH)(CO)$_3$Cl (200 mg, 0.385 mmol, 1.0 equiv) and KSCN (3.73 g, 38.5 mmol, 100 equiv) were combined in a flask with 20 mL of 1:1 95% ethanol/water and refluxed overnight under N_2. The ethanol was removed in vacuo, and the mixture was extracted with ethyl acetate. The various extracts were combined, dried over $MgSO_4$, and the solvent was removed in vacuo to furnish a red powder (136 mg, 65%). ^{1}H NMR (300 MHz, d-acetone, 25 °C): δ = 2.70 (s, 3H, bpy-CH$_3$), 7.73 (d, 1H, bpy-H), 8.28 (m, 1H, bpy-H), 8.87 (s, 1H, bpy-H), 8.99 (d, 1H, bpy-H), 9.07 (s, 1H, bpy-H), 9.33 (d, 1H, bpy-H). Anal. Calcd for $C_{16}H_{10}N_3O_5ReS$: C, 35.42; H, 1.86; N, 7.75; S, 5.91. Found: C, 35.35; H, 1.81; N, 7.71; S, 5.97.

Tricarbonylcyano(4′-methyl-2,2′-bipyridine-4-carboxylic acid)-rhenium(I) (Re(bpy-COOH)(CO)$_3$CN). Re(bpy-COOH)(CO)$_3$Cl (200 mg, 0.385 mmol, 1.0 equiv) and NaCN (1.89 g, 38.5 mmol, 100 equiv) were combined in a round-bottom flask with 40 mL of 1:1 95% ethanol/water, and the mixture was heated at reflux for 6 h. The ethanol was removed in vacuo, yielding a bright yellow precipitate, which was isolated by filtration, washed with copious amounts of water and ether, and dried under vacuum (168 mg, 86%). ^{1}H NMR (300 MHz, CD$_3$-OD, 25 °C): δ = 2.63 (s, 3H, bpy-CH$_3$), 7.54 (d, 1H, bpy-H), 8.03 (m, 1H, bpy-H), 8.49 (s, 1H, bpy-H), 8.89 (m, 2H, bpy-H), 9.08 (d, 1H, bpy-H). Anal. Calcd for $C_{16}H_{10}N_3O_5Re$: C, 37.65; H, 1.97; N, 8.23. Found: C, 37.53; H, 2.06; N, 8.20.

4′-Methyl-2,2′-bipyridine-4-alanine *tert*-butyl ester (bpy-A-O*t*Bu). Bpy-COOH (0.502 g, 2.34 mmol, 1.0 equiv), A-O*t*Bu·HCl (0.425 g, 2.34 mmol, 1.0 equiv), WSC·HCl (0.493 g, 2.57 mmol, 1.1 equiv), and HOBt (0.374 g, 2.57 mmol, 1.1 equiv) were combined in a round-bottom flask. CH_2Cl_2 (100 mL) and NMM (1 mL, 9.4 mmol, 4 equiv) were added, and the reaction mixture was stirred overnight. The reacted solution was washed in a separatory funnel with 2 × 50 mL of water, 10% citric acid, and 1.0 M $NaHCO_3$, and the organic layer was collected and dried over $MgSO_4$. The solvent was removed in vacuo to yield an oil, which solidified under high vacuum as a white mass (0.5947 g, 57%). ^{1}H NMR (300 MHz, $CDCl_3$, 25 °C): δ =1.47 (m, 12H, *t*Bu and A-CH$_3$), 2.45 (s, 3H, bpy-CH$_3$), 4.72 (m, 1H, A-CH), 7.07 (d, 1H, N-H), 7.15 (d, 1H, bpy-H), 7.70 (d, 1H, bpy-H), 8.25 (s, 1H, bpy-H), 8.55 (d, 1H, bpy-H), 8.70 (s, 1H, bpy-H), 8.78 (d, 1H, bpy-H).

4′-Methyl-2,2′-bipyridine-4-tyrosine *tert*-butyl ester (bpy-Y-O*t*Bu). Bpy-COOH (0.750 g, 3.50 mmol, 1.0 equiv), Y-O*t*Bu (0.830 g, 3.50 mmol, 1.0 equiv), WSC·HCl (0.738 g, 3.85 mmol, 1.1 equiv), HOBt (0.520 g, 3.85 mmol, 1.1 equiv), and DMAP (43 mg, 0.35 mmol, 0.1 equiv) were combined in a round-bottom flask. Methylene chloride (CH_2Cl_2, 200 mL) and NMM (1.7 mL, 15.4 mmol, 4.4 equiv) were added, and the reaction mixture was stirred overnight. The reacted solution was washed in a separatory funnel with 4 × 100 mL of water, and the organic layer was collected and dried over $MgSO_4$. The solvent was removed in vacuo to yield a yellow oil, which under high vacuum, produced an off-white solid. The solid was dissolved in a few milliliters of ethyl acetate, loaded onto a Chromatotron plate (alumina, 2 mm), and eluted with ethyl acetate. The first band to elute was collected and the solvent removed in vacuo to yield an oil, which solidified under high vacuum as an off-white solid (0.5921 g, 39%). ^{1}H NMR (300 MHz, $CDCl_3$, 25 °C): δ =1.47 (s, 9H, *t*Bu), 2.45 (s, 3H, bpy-CH$_3$), 3.16 (m, 2H, Y-CH$_2$), 4.96 (m, 1H, Y-CH), 6.68 (d, 2H, phenol-H), 7.02 (m, 2H, phenol-H and bpy-H), 7.17 (d, 1H, N-H), 7.70 (m, 1H, bpy-H), 8.23 (s, 1H, bpy-H), 8.53 (d, 1H, bpy-H), 8.63 (s, 1H, bpy-H), 8.78 (d, 1H, bpy-H).

Tricarbonylchloro(4′-methyl-2,2′-bipyridine-4-alanine *tert*-butyl ester)rhenium(I) (Re(bpy-A-O*t*Bu)(CO)$_3$Cl). Re(CO)$_5$Cl (500 mg, 1.38 mmol, 1.0 equiv) and bpy-A-O*t*Bu (471 mg, 138 mmol, 1.0 equiv) were combined in a round-bottom flask with 50 mL of toluene, and the mixture was heated at reflux overnight. The yellow suspension was cooled in an ice bath, and the yellow solid was isolated by filtration, washed with ether, and dried under vacuum (722 mg, 81%). ^{1}H NMR (300 MHz, d-acetone, 25 °C): δ = 1.47 (m, 12H, *t*Bu), 2.59 (s, 3H, bpy-CH$_3$), 4.41 (m, 1H, Y-CH), 7.61 (d, 1H, bpy-H), 8.02 (m, 1H, bpy-H), 8.70 (s, 1H, bpy-H), 8.85 (d, 1H, bpy-H), 8.95 (s, 1H, bpy-H), 9.13 (d, 1H, bpy-H), 9.31 (m, 1H, N-H) Anal. Calcd for $C_{22}H_{23}ClN_3O_6Re$: C, 40.83; H, 3.58; N, 6.49. Found: C, 40.96; H, 3.72; N, 6.52.

Tricarbonylchloro(4′-methyl-2,2′-bipyridine-4-tyrosine *tert*-butyl ester)rhenium(I) (Re(bpy-Y-O*t*Bu)(CO)$_3$Cl). Re(CO)$_5$Cl (467 mg, 1.29 mmol, 1.0 equiv) and bpy-Y-O*t*Bu (560 mg, 1.29 mmol, 1.0 equiv) were combined in a round-bottom flask with 50 mL of toluene, and the mixture was heated at reflux overnight. The yellow suspension was cooled in an ice bath, and the yellow solid was isolated by filtration, washed with ether, and dried under vacuum (668 mg, 70%). ^{1}H NMR (300 MHz, d-acetone, 25 °C): δ = 1.36 (s, 9H, *t*Bu), 2.58 (s, 3H, bpy-CH$_3$), 3.01 (m, 2H, Y-CH$_2$), 4.57 (m, 1H, Y-CH), 6.66 (d, 2H, phenol-H), 7.08 (d, 2H, phenol-H), 7.61 (d, 1H, bpy-H), 7.97 (m, 1H, bpy-H), 8.65 (s, 1H, bpy-H), 8.86 (m, 2H, bpy-H), 9.17 (m, 1H, bpy-H), 9.33 (m, 1H, N-H) Anal. Calcd for $C_{28}H_{27}ClN_3O_7Re$: C, 45.50; H, 3.68; N, 5.68. Found: C, 45.36; H, 3.75; N, 5.74.

Tricarbonylthiocyanato(4′-methyl-2,2′-bipyridine-4-tyrosine *tert*-butyl ester)rhenium (I) (Re(bpy-Y−O*t*Bu)(CO)$_3$SCN). Re(bpy-Y-O*t*Bu)(CO)$_3$Cl (111 mg, 0.150 mmol, 1.0 equiv) and KSCN (1.46 g, 15 mmol, 100 equiv) were combined in a round-bottom flask with 40 mL of 1:1 95% ethanol/water and heated at reflux overnight. The ethanol was removed in vacuo, and the red precipitate was isolated by filtration, washed with copious amounts of water, and dried under high vacuum (91 mg, 80%). ^{1}H NMR (300 MHz, d-acetone, 25 °C): δ = 1.45 (s, 9H, *t*Bu), 2.70 (s, 3H, bpy-CH$_3$), 4.87 (m, 1H, Y-CH), 6.79 (m, 2H, phenol-CH$_2$), 7.19 (m, 2H, phenol-CH$_2$), 7.73 (m, 1H, bpy-H), 8.12 (m, 1H, bpy-H), 8.46 (d, 1H, N-H), 8.69 (m, 1H, bpy-H), 8.90 (m, 1H, bpy-H), 8.98 (m, 1H, bpy-H), 9.25 (m, 1H, bpy-H).

Tricarbonylcyano(4′-methyl-2,2′-bipyridine-4-phenylalanine)rhenium(I) (Re(bpy-F)(CO)$_3$CN). Re(bpy-COOH)(CO)$_3$(CN) (130 mg, 0.321 mmol, 1.0 equiv), F-O*t*Bu·HCl (72 mg, 0.321 mmol, 1.0 equiv), WSC·HCl (53 mg, 0.353 mmol, 1.1 equiv), and HOBt (37 mg, 0.353 mmol, 1.1 equiv) were combined in a round-bottom flask with 25 mL of DMF. NMM (0.12 mL, 4.0 equiv) was added, and the mixture was stirred overnight. The solvent was removed in vacuo, and the resulting yellow oil was dissolved in 100 mL of CH_2Cl_2 and washed with 2 × 25 mL water, 10% citric acid, 1.0 M $NaHCO_3$, and water in that order. The organic phase, isolated with a separatory funnel, was dried over $MgSO_4$, and the solvent was removed in vacuo. The resulting yellow solid was dissolved in 10 mL of 1:1 TFA/CH_2Cl_2 and stirred for 1 h. The solution was concentrated to <1 mL under a stream of N_2 and triturated with ether. The bright yellow solid that precipitated was isolated by filtration, washed with copious amounts of ether, and dried under vacuum (82 mg, 39%). ^{1}H NMR (300 MHz, CD$_3$OD, 25 °C): δ = 2.64 (s, 3H, bpy-CH$_3$), 3.13 (m, 2H, F-CH$_2$), 4.96 (m, 1H, F-CH), 7.30 (m, 5H, F-ph), 7.57 (m, 1H, bpy-H), 7.86 (m, 1H, bpy-H), 8.49 (m, 1H, bpy-H), 8.79 (m, 1H, bpy-H), 8.89 (m, 1H, bpy-H), 9.14 (m, 1H, bpy-H). Anal. Calcd for $C_{25}H_{19}N_4O_6Re$: C, 45.66; H, 2.91; N, 8.52. Found: C, 45.48; H, 2.85; N, 8.42.

Tricarbonylcyano(4′-methyl-2,2′-bipyridine-4-tyrosine)rhenium-(I) (Re(bpy-Y)(CO)$_3$(CN)). The synthesis of the tyrosine derivative was the same as that for the phenylalanine derivative, except that Re-(CO)$_3$(bpy-COOH)(CN) (193 mg, 0.377 mmol, 1.0 equiv), WSC·HCl (80 mg, 0.415 mmol, 1.1 equiv), and HOBt (43 mg, 0.415 mmol, 1.1 equiv) were combined with Y-O*t*Bu (90 mg, 0.377 mmol, 1.0 equiv), instead of F-O*t*Bu·HCl (49%). ^{1}H NMR (300 MHz, CD$_3$OD, 25 °C): δ = 2.64 (s, 3H, bpy-CH$_3$), 3.03 (m, 2H, Y-CH$_2$), 4.87 (m, 1H, F-CH), 6.71 (d, 2H, phenol-H), 7.11 (d, 2H, phenol-H), 7.57 (m, 1H, bpy-H), 7.87 (m, 1H, bpy-H,), 8.48 (m, 1H, bpy-H), 8.76 (m, 1H, bpy-H), 8.89 (m, 1H, bpy-H), 9.15 (m, 1H, bpy-H). Anal. Calcd for $C_{25}H_{19}N_4O_7Re$: C, 44.57; H, 2.84; N, 8.23. Found: C, 44.42; H, 2.76; N, 8.17.

Tricarbonyl(acetonitrile)(1,10-phenanthroline)rhenium(I) Hexafluorophosphate ([Re(phen)(CO)$_3$(CH$_3$CN)](PF$_6$)). Re(phen)(CO)$_3$Cl (400 mg, 0.823 mmol, 1.0 equiv) and TlPF$_6$ (374 mg, 1.07 mmol, 1.3 equiv) were combined in a round-bottom flask with 40 mL of CH$_3$CN and heated at reflux in the dark overnight. The solvent was removed in vacuo, leaving a yellow oil, which was dissolved in CH$_2$Cl$_2$. Any remaining solids were filtered off, and ether was slowly dripped into the solution to produce long yellow/green luminescent crystals, which were isolated by filtration, washed with ether, and dried under vacuum (450 mg, 86%). ^{1}H NMR (300 MHz, d-acetone, 25 °C): δ = 2.17 (s, 3H, CH$_3$CN-Re), 8.27 (m, 2H, phen-H), 8.42 (m, 2H, phen-H), 9.11 (d, 2H, phen-H), 9.63 (d, 2H, phen-H). Anal. Calcd C$_{17}$H$_{11}$F$_6$N$_3$O$_3$PRe: C, 32.08; H, 1.74; N, 6.60. Found: C, 32.15; H, 1.66; N, 6.47.

Tricarbonyl(diphenylphosphinobenzoic acid)(1,10-phenanthroline)rhenium(I) Hexafluorophosphate ([Re(phen)(Ph$_2$PPh-COOH)(CO)$_3$](PF$_6$)). [Re(phen)(CO)$_3$(CH$_3$CN)](PF$_6$ (877 mg, 1.37 mmol, 1.0 equiv) and Ph$_2$PPh-COOH (633 mg, 2.07 mmol, 1.5 equiv) were combined in a round-bottom flask with 40 mL of N$_2$-purged acetone. The solution was heated at reflux overnight under a N$_2$ atmosphere in the dark. The solvent was removed in vacuo without heating, and the yellow solid was taken up in CH$_2$Cl$_2$. The resulting light yellow precipitate was isolated by filtration and washed with CH$_2$Cl$_2$ (1.118 g, 90%). ^{1}H NMR (300 MHz, d-acetone, 25 °C): δ = 7.05−7.80 (m, 14H, Ph$_2$PPh-R), 8.02 (m, 2H, phen-H), 8.27 (s, 2H, phen-H), 8.90 (d, 2H, phen-H), 9.44 (d, 2H, phen-H). MALDI-TOF calcd (found): [M − PF$_6$]$^+$ 757.09 (757.03); [M − CO,PF$_6$]$^+$ 729.10 (729.05). Anal. Calcd C$_{34}$H$_{23}$F$_6$N$_2$O$_5$P$_2$Re: C, 45.29; H, 2.57; N, 3.11. Found: C, 45.21; H, 2.63; N, 3.06.

[Re(phen)(P-Y)(CO)$_3$](PF$_6$). Re(phen)(CO)$_3$(Ph$_2$PPh-COOH)](PF$_6$) (200 mg, 0.222 mmol, 1.0 equiv), Y-O*t*Bu (53 mg, 0.222 mmol, 1.0 equiv), WSC·HCl (47 mg, 0.244 mmol, 1.1 equiv), HOBt (33 mg, 0.244 mmol, 1.1 equiv), and NMM (100 μL, 0.888 mmol, 4.0 equiv) were combined in a round-bottom flask with 20 mL of CH$_2$Cl$_2$ and stirred overnight. The solution was diluted with 50 mL of CH$_2$Cl$_2$, washed with 2 × 25 mL of water, and dried over MgSO$_4$. The solution was concentrated to a few milliliters in vacuo and loaded onto a silica gel Chromatotron plate (2 mm). The highly emissive band that eluted with 5% MeOH/CH$_2$Cl$_2$ was collected and the solvent removed in vacuo to yield a yellow solid, which was dissolved in 10 mL of 1:1 TFA/CH$_2$Cl$_2$ and stirred for 1 h. The solution was concentrated under a stream of N$_2$. Addition of ether caused a yellow solid to precipitate; the solid was isolated by filtration and dried under vacuum (140 mg, 59%). ^{1}H NMR (300 MHz, d-acetone, 25 °C): δ = 3.18 (m, 2H, Y-CH$_2$), 4.89 (s, 1H, Y-CH), 6.85 (d, 2H, phenol-H), 7.20 (d, 2H, phenol-H), 7.27−7.85 (m, 14H, Ph$_2$-P-Ph-R), 7.98 (m, 2H, phen-H), 8.14 (s, 2H, phen-H), 8.80 (m, 2H, phen-H), 9.42 (m, 2H, phen-H). ^{31}P NMR (300 MHz, d-acetone, 25 °C): δ = 19.5 (s, Re-P). MALDI-TOF calcd (found): [M − PF$_6$]$^+$ 920.15 (920.05); [M − CO,PF$_6$]$^+$ 892.16 (892.07). Anal. Calcd C$_{43}$H$_{32}$F$_6$N$_3$O$_7$P$_2$Re: C, 48.50; H, 3.03; N, 3.95. Found: C, 48.42; H, 2.95; N, 4.06.

[Re(phen)(P-F)(CO)$_3$](PF$_6$). The synthesis of the phenylalanine derivative was the same as that for the tyrosine derivative, except that F-O*t*Bu·HCl was used instead of Y-O*t*Bu (74%). ^{1}H NMR (300 MHz, d-acetone, 25 °C): δ = 3.29 (m, 2H, F-CH$_2$), 4.93 (m, 1H, F-CH), 6.72−7.54 (m, 19H, F-phenyl and Ph$_2$PPh-R), 7.97 (m, 2H, phen-H), 8.14 (s, 2H, phen-H), 8.81 (m, 2H, phen-H), 9.43 (m, 2H, phen-H). ^{31}P NMR (300 MHz, d-acetone, 25 °C): δ = 19.3 (s, Re-P). MALDI-TOF calcd (found): [M − PF$_6$]$^+$ 904.16 (903.94); [M − CO,PF$_6$]$^+$ 876.16 (875.98). Anal. Calcd C$_{43}$H$_{32}$F$_6$N$_3$O$_6$P$_2$Re: C, 49.24; H, 3.08; N, 4.01. Found: C, 49.18; H, 3.04; N, 3.96.

Re(PP-Bn)(CO)$_3$Cl. Re(CO)$_5$Cl (126 mg, 0.14 mmol, 1.0 equiv) and HOOC-PP-Bn (200 mg, 0.174 mmol, 1.0 equiv) were combined in a flask with 25 mL of N$_2$-purged toluene, and the mixture was heated at reflux under N$_2$ overnight. The solution was concentrated to a few milliliters in vacuo and triturated with hexanes. The white precipitate was isolated by filtration, washed with hexanes, and dried under vacuum (0.258 g). The crude product, which contained some Re(HOOC-PP-Bn)(CO)$_3$Cl, was used in the next step without further purification. MALDI-TOF calcd (found): [M − Cl]$^+$ 800.11 (800.22).

[Re(phen)(PP-Bn)(CO)$_2$](PF$_6$). Re(PP-Bn)(CO)$_3$Cl (150 mg, 0.171 mmol, 1.0 equiv), phen (34 mg, 0.188 mmol, 1.1 equiv), and TlPF$_6$ (64 mg, 0.188 mmol, 1.1 equiv) were combined in a round-bottom flask with 25 mL of anhydrous *o*-dichlorobenzene. The mixture was bubbled with N$_2$ for 30 min and heated at reflux for 5 h under N$_2$. The dark yellow solution was filtered over Celite, which was rinsed with CH$_2$Cl$_2$. The solvent was then removed from the filtrate in vacuo; the residue was dissolved in a minimal volume of CH$_2$Cl$_2$ and loaded onto a Chromatotron plate (alumina, 1 mm). The product eluted with 10% CH$_3$CN/CH$_2$Cl$_2$ as a golden yellow band. The solvent was removed in vacuo, yielding a yellow solid, which was characterized as a mixture of two isomers. ^{31}P NMR (300 MHz, CDCl$_3$, 25 °C): δ = 35.3 (d), 44.0 (d), 49.9 (d), 60.9 (d). MALDI-TOF calcd (found): [M − PF$_6$]$^+$ 952.19 (952.25); [M − CO,PF$_6$]$^+$ 924.19 (924.25).

X-ray Crystal Structure of [Re(phen)(dppe)(CO)$_2$](PF$_6$) and [Re(phen)(PP-Bn)(CO)$_2$](PF$_6$)·CDCl$_3$. Single crystals of the complexes were grown by slow evaporation from a concentrated solution in CDCl$_3$. A crystal was removed from the supernatant, coated with Paratone N oil, and mounted on a glass fiber. X-ray diffraction data were collected at −123 °C on a Siemens diffractometer equipped with a CCD detector, using the Mo Kα radiation. The data were integrated to *hkl* intensity, and the unit cell was calculated using the SAINT version 4.050 program from Siemens. Solution and refinement were performed by direct methods (SHELXTL version 6.10, Sheldrick, G. M., and Siemens Industrial Automation, Inc., 2000). The structures were solved by the Patterson method; non-hydrogen atoms were refined anisotropically, and hydrogen atoms were placed at calculated positions. Figure S1 and Tables S1−S6 contain details regarding the refined data, cell parameters, and results of the solution of the X-ray diffraction data of [Re(phen)(PP-Bn)(CO)$_2$](PF$_6$)·CDCl$_3$; similar data accompanying the X-ray crystal structure of [Re(phen)(dppe)(CO)$_2$](PF$_6$) are presented in Figure S2 and Tables S7−S12 of the Supporting Information.

Physical Measurements. ^{1}H and ^{31}P NMR spectra were recorded on a Varian Mercury 300 MHz NMR at the MIT Department of Chemistry Instrumentation Facility (DCIF) and externally referenced to tetramethylsilane (^{1}H) and phosphoric acid (^{31}P). MALDI-TOF mass spectrometry was performed on a Bruker Omniflex instrument in the DCIF using dithranol as the matrix. The instrument was calibrated with a quadratic polynomial using a mixture of bradykinin fragment 1−7 (757.3997), angiotensin II (1046.5423), and P14R synthetic peptide (1533.8582) (Sigma) with α-cyano-4-hydroxycinnamic acid as the matrix. Elemental analysis was performed by H. Kolbe Mikroanalytisches Laboratorium in Mülheim an der Ruhr, Germany.

UV−vis absorption spectra were recorded on a Cary 17D modified by On-Line Instrument Systems (OLIS) to include computer control or a Spectral Instruments 440 spectrophotometer. Steady-state emission spectra were recorded on an automated Photon Technology International (PTI) QM 4 fluorimeter equipped with a 150 W Xe arc lamp and a Hamamatsu R928 photomultiplier tube. Time-resolved emission and transient absorption (TA) measurements on the >20 ns time scale were made with pump light provided by the third harmonic (355 nm) of an Infinity Nd:YAG laser (Coherent) running at 20 Hz as previously described.[44] Time-resolved emission measurements on the <20 ns time scale were made with the frequency doubled (400 nm) pump light provided by a Ti:sapphire laser system (100 fs pulse width) and collected on a Hamamatsu C4334 Streak Scope streak camera as previously described.[16]

The corrected emission spectra were analyzed by a standard Franck−Condon analysis:[45−47]

$$I(\bar{\nu}) = \sum_{\upsilon=0}^{5} \left\{ \left(\frac{E_0 - \upsilon\hbar\omega}{E_0} \right)^3 \left(\frac{S^\upsilon}{\upsilon!} \right) \exp\left[-4\ln 2 \left(\frac{\bar{\nu} - E_0 + \upsilon\hbar\omega}{\Delta\bar{\nu}_{1/2}} \right)^2 \right] \right\} \quad (1)$$

Scheme 1 [a]

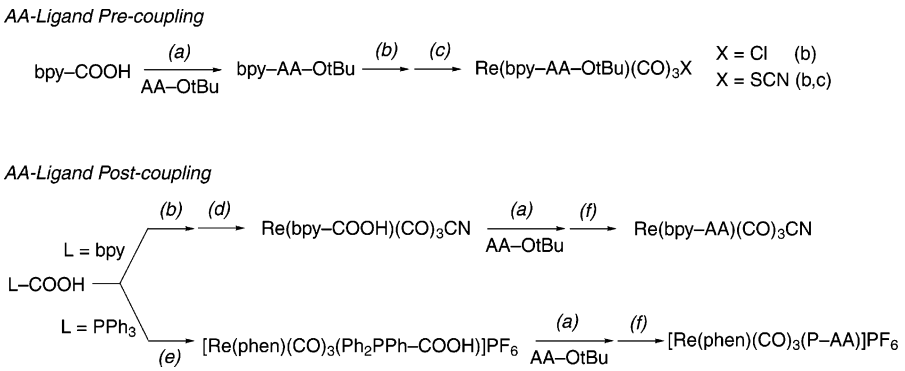

[a] Conditions: (a) WSC·HCl, HOBt, NMM, CH_2Cl_2; (b) $Re(CO)_5Cl$, △, toluene; (c) KSCN, EtOH; H_2O (1:1); (d) NaCN, EtOH:H_2O(1:1); (e) $[Re(phen)(CO)_3(MeCN)]PF_6$, acetone; (f) TFA:$CH_2Cl_2$(1:1).

in which $I(\bar{\nu})$ is the corrected emitted intensity in quanta ($I(\lambda) \times \lambda^2$). The other parameters of eq 1 have been described elsewhere.[46,47] The E_0, S, frequency ($\hbar\omega$), and bandwidth ($\Delta\bar{\nu}_{1/2}$) values for the emission spectra were obtained by fitting the emission bands to eq 1 using Microcal Origin. Without a direct and independent measure of these parameters, the fit is overparametrized, and the values obtained are, at best, an approximation. Relative quantum yields of samples, Φ_{sam}, were calculated using $[Ru(bpy)_3](PF_6)_2$ in CH_3CN and water as the reference actinometer according to

$$\Phi_{sam} = \Phi_{ref}\left(\frac{A_{ref}}{A_{sam}}\right)\left(\frac{I_{sam}}{I_{ref}}\right)\left(\frac{\eta_{sam}}{\eta_{ref}}\right)^2 \qquad (2)$$

Φ_{ref} is the emission quantum yield of the $Ru(bpy)_3^{2+}$ reference taken to be 0.062 in CH_3CN[48] and 0.053 in water.[49] A is the measured absorbance; η is the refractive index of the solvent, and I is the integrated emission intensity, which was obtained by plotting and integrating the entire emission band fitted using eq 1. Samples for phosphorescence quantum yield and time-resolved spectroscopic measurements were freeze−pump−thaw degassed for five cycles to 10^{-6} Torr. Unless otherwise noted, all spectroscopy was performed in 10 mM aqueous phosphate buffer with the pH adjusted using 1 M NaOH or HCl. In cases of limited solubility, the samples were sonicated in a Branson 3200 sonicator and filtered through a 0.2 micron Gelman Acrodisc polypropylene syringe filter prior to measurement.

Electrochemical measurements were performed using a Bioanalytical Systems (BAS) Model CV-50W potentiostat/galvanostat. Differential pulse voltammetry (DPV) was performed using a platinum disk working electrode, a Ag/AgCl reference electrode, and a platinum wire auxiliary electrode. DPV experiments were performed in dry CH_3CN with 0.1 M tetrabutylammonium hexafluorophosphate $(Bu_4N)PF_6$ as the supporting electrolyte, and solutions were bubbled with Ar to remove dissolved O_2. All potentials are reported versus $E°(Fc^+/Fc) = 0.65$ V versus NHE in CH_3CN.[50] Spectroelectrochemistry was performed in dry DMF with 0.1 M $(Bu_4N)PF_6$ as the supporting electrolyte and Pt gauze as the working electrode in a 2 mm path length quartz optical cell. A blank spectrum was recorded on the solution prior to electrolysis at −1.65 V versus Fc^+/Fc. Spectra were recorded every 10 s for 5 min.

Results

Synthesis. Scheme 1 highlights the two approaches undertaken in the syntheses of the amino acid containing Re^I complexes. The Re(bpy-AA-O*t*Bu)$(CO)_3(X)$ complexes (AA = amino acid, A, and Y; X = Cl^-, SCN^-) were prepared by precoupling the *tert*-butyl ester protected amino acid to the carboxylic acid of the bpy ligand using standard peptide coupling conditions. This modified bpy ligand was then added to the appropriate Re^I synthon, followed by deprotection of the amino acid with trifluoroacetic acid. We note that these deprotection conditions led to scrambling of the ^1H NMR peaks in the bpy−aryl region, and biexponential emission decay lifetimes were observed for the acid-treated material. These results are consistent with an exchange of the X^- ligand by the deprotected carboxylate of the coupled amino acid. Similar complexes, $Re(phen)(CO)_3(L)^+$ (L = pyridine, imidazole, His), have previously been shown to exchange L for carboxylate in reactions with acetic acid and/or synthetically appended carboxylate groups.[51] For the preparation of Re(bpy-AA-O*t*Bu)-$(CO)_3(CN)$ (AA = F and Y), exchange of X = Cl^- by CN^- did not proceed cleanly in the precoupling synthesis scheme, and thus this method was abandoned. Instead, we found that a post-coupling strategy proved to be more synthetically feasible, in which bpy-COOH was first complexed to a Re^I synthon employing methods used to obtain other $Re(NN)(CO)_3Cl$ (NN = polypyridyl) complexes.[52] The Cl^- anion was then exchanged for CN^- and the amino acid coupled to the Re(bpy-COOH)-$(CO)_3(CN)$ complex. Unlike the X = Cl^- and SCN^- derivatives, the X = CN^- derivative proved to be inert to carboxylate exchange under the conditions of amino acid deprotection, thus enabling the isolation of pure $Re(bpy\text{-}AA)(CO)_3(CN)$ compounds for spectroscopic study.

The amide linkage required for amino acid modification is furnished from carboxylic acid-containing phosphine ligands of the analogous monodentate (P) $Re(NN)(P)(CO)_3^+$ [53−56] and

(44) Loh, Z.-H.; Miller, S. E.; Chang, C. J.; Carpenter, S. D.; Nocera, D. G. *J. Phys. Chem. A* **2002**, *106*, 11700.
(45) Caspar, J. V.; Meyer, T. J. *J. Am. Chem. Soc.* **1983**, *105*, 5583.
(46) Chen, P.; Meyer, T. J. *Chem. Rev.* **1998**, *98*, 1439.
(47) Striplin, D. R.; Reece, S. Y.; McCafferty, D. G.; Wall, C. G.; Friesen, D. A.; Erickson, B. W.; Meyer, T. J. *J. Am. Chem. Soc.* **2004**, *126*, 5282.
(48) Calvert, J. M.; Caspar, J. V.; Binstead, R. A.; Westmoreland, T. D.; Meyer, T. J. *J. Am. Chem. Soc.* **1982**, *104*, 6620.
(49) Henderson, L. J., Jr.; Cherry, W. R. *J. Photochem.* **1985**, *28*, 143.
(50) Connelly, N. G.; Geiger, W. E. *Chem. Rev.* **1996**, *96*, 877.
(51) Chang, M. C. Y. Ph.D. Thesis, Massachusetts Institute of Technology, 2003.
(52) Caspar, J. V.; Meyer, T. J. *J. Phys. Chem.* **1983**, *87*, 952.
(53) Caspar, J. V.; Sullivan, B. P.; Meyer, T. J. *Inorg. Chem.* **1984**, *23*, 2104.
(54) Hori, H.; Koike, K.; Ishizuka, M.; Takeuchi, K.; Ibusuki, T.; Ishitani, O. *J. Organomet. Chem.* **1997**, *530*, 169.
(55) Koike, K.; Tanabe, J.; Toyama, S.; Tsubaki, H.; Sakamoto, K.; Westwell, J. R.; Johnson, F. P. A.; Hori, H.; Saitoh, H.; Ishitani, O. *Inorg. Chem.* **2000**, *39*, 2777.
(56) Koike, K.; Okoshi, N.; Hori, H.; Takeuchi, K.; Ishitani, O.; Tsubaki, H.; Clark, I. P.; George, M. W.; Johnson, F. P. A.; Turner, J. J. *J. Am. Chem. Soc.* **2002**, *124*, 11448.

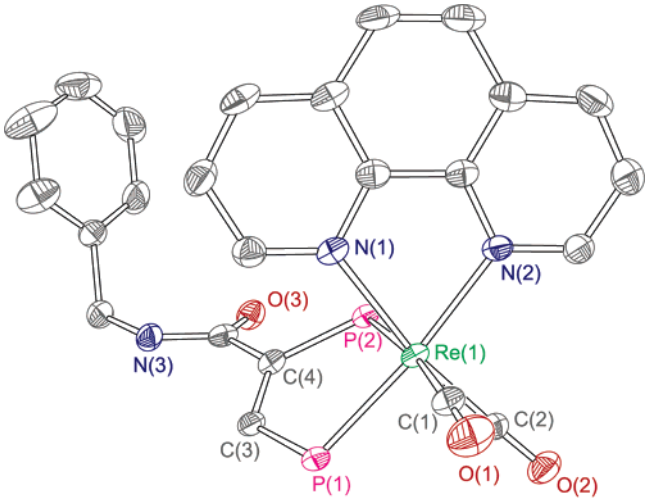

Figure 1. Thermal ellipsoid plot of a single isomer of [Re(phen)(PP-Bn)-$(CO)_2$]PF_6·$CDCl_3$ shown at 50% probability. The PF_6^- anion, the solvent molecule, and the phosphine phenyl groups have been removed for clarity.

bidentate (PP) Re(NN)(PP)$(CO)_2^+$ [40] complexes. The parent complex, [Re(phen)(dppe)$(CO)_2$](PF_6), originally synthesized by Schutte et al.,[40] has been obtained in single crystal form and structurally characterized by X-ray diffraction (Figure S2, Tables S7−S12). The dppe analogue can be derivatized by introducing carboxylic acid functionality on the ethylene backbone in the protected form as the 2,3-bis(diphenylphosphino)maleic anhydride (bma). An amide bond linkage has been established by nucleophilically attacking bma with benzylamine.[42] This amide functionalized ligand was adapted to Re^I coordination chemistry by reacting it with $Re(CO)_5Cl$ and subsequently chelating with phen to yield the model complex, [Re(phen)(PP-Bn)$(CO)_2$](PF_6). The extra carboxylic acid group, which remained on the Bn-PP-COOH ligand upon ring opening the anhydride, was observed to decarboxylate with the application of the heat required for subsequent PP and phen chelation. The crystal structure of one geometric isomer of [Re(phen)(PP-Bn)$(CO)_2$]-(PF_6), shown in Figure 1, confirms the formation of the crucial amide bond to one carboxylic acid and the decarboxylation of the other. The two CO ligands adopt a *cis* stereochemistry, and the phosphorus atom on the derivatized side of the chelating ligand is *trans* to CO. The other isomer, which did not crystallize, has this phosphorus *trans* to the nitrogen of phen. Tables S3 and S4 list the bond lengths and angles, respectively, obtained from the solution of the X-ray structure. The bite angles of the PP-Bn and phen ligands ($\angle$P(1)−Re(1)−P(2) = 80.72° and $\angle$N(1)−Re(1)−N(2) = 75.37°) create a distorted octahedral coordination geometry. The Re−C bond distances are slightly longer (d(Re−C) = 1.902 and 1.928 Å) and the C−O bond distances slightly shorter (d(C−O) = 1.169 and 1.164 Å) than a crystallographically characterized relative, $Re(CO)_2(P(OEt)_3)$-(PPh_3)(4,4′-Me_2-2,2′-bpy)$^+$, which features two monodentate phosphine ligands *trans* to one another (d(Re−C) = 1.84(3) and 1.88(3) Å; d(C−O) = 1.18(4) and 1.17(3) Å).[55]

The carboxylic acid derivatives of the monodentate and bidentate phosphines can be modified with amino acids. We present the chemistry of only the former owing to their greater water solubility and higher MLCT energy (vide infra). The [Re-(phen)(P-AA)$(CO)_3$](PF_6) (AA = F and Y) complexes were synthesized using the AA-ligand post-coupling strategy of Scheme 1. These compounds were inert to carboxylate exchange upon amino acid deprotection, as exhibited by the single, downfield shifted peak in the ^{31}P NMR spectrum (versus free phosphine), satisfactory MALDI-TOF and elemental analysis, and the single-exponential behavior of the emission decay (vide infra).

Table 1. Spectroscopic and Photophysical Properties of the MLCT Excited State of Re^I Polypyridyl Carbonyl Complexes in Aqueous Solution at Room Temperature

complex	E_{abs} (cm^{-1})	E_{em} (cm^{-1})[a]	Φ_{em}[a]	τ_{em} (ns)[a]
Re(bpy-COOH)$(CO)_3$Cl	~28500	15700	1.1×10^{-3}	5.5
Re(bpy-COOH)$(CO)_3$SCN	27400	15100	1.6×10^{-3}	12.0
Re(bpy-COOH)$(CO)_3$CN	28600	16400	1.4×10^{-2}	86.5
Re(bpy-F)$(CO)_3$CN	27900	15800		59.4
[Re(phen)(P-F)$(CO)_3$](PF_6)	27100	19100	9.4×10^{-2}	3900
[Re(phen)(dppe)$(CO)_2$](PF_6)[b]	~27000	16300	7.8×10^{-2}	3200
[Re(phen)(PP-Bn)$(CO)_2$](PF_6)[b,c]				940

[a] λ_{exc} = 355 nm. [b] CH_3CN solvent. [c] Isomer shown in Figure 1. Isolated solids from synthesis exhibit biexponential behavior arising from the presence of the two isomers (see text).

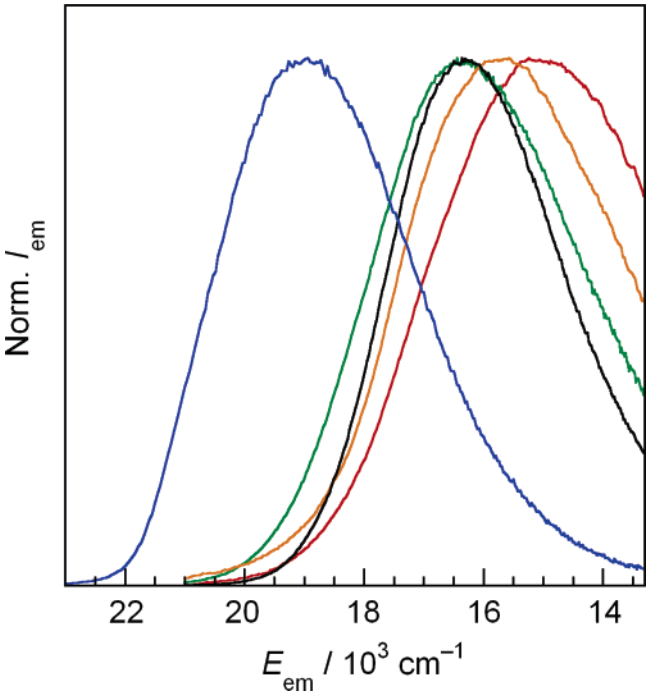

Figure 2. Normalized, corrected emission spectra for Re(bpy-COOH)-$(CO)_3$(X) [X = CN^- (green line), Cl^- (orange line), SCN^- (red line)] and [Re(phen)(P-F)$(CO)_3$](PF_6) (blue line) in 10 mM phosphate buffer at pH 7 and [Re(phen)(dppe)$(CO)_2$](PF_6) (black line) in CH_3CN.

Photophysics. The spectroscopic properties for the Re^I polypyridyl carbonyl complexes are summarized in Table 1. The MLCT transition for the Re^I polypyridyl carbonyl complexes appears as a shoulder on the strong $\pi \rightarrow \pi^*$ absorption profile of the polypyridyl ligand. As has been observed previously,[56] the MLCT absorption band of the biscarbonyl complexes is red shifted from that of their tricarbonyl counterparts. Excitation into the MLCT absorbance manifold produces the broad, structureless emission bands shown in Figure 2, where the intensity has been scaled in quanta ($I \times \lambda^2$) and normalized.

The emission maximum (E_{em}) of Re(bpy-COOH)$(CO)_3$(X) decreases across the series X = CN^- > Cl^- > SCN^-. Derivatization of the bpy ligand with an amino acid causes a red shift of the MLCT emission, as evidenced from the

comparison of the Re(bpy-COOH)$(CO)_3$(CN) and Re(bpy-F)-$(CO)_3$(CN) emission maxima in Table 1. Numerous studies of the room temperature emission properties of $Re^I(NN)(CO)_3L^+$ complexes establish the emission to be of ^{3}MLCT parentage.[57] A more detailed analysis of $Re^I(NN)(CO)_3Cl$ photophysics reveals that the MLCT emission arises from three states of triplet orbital parentage in thermal equilibrium at room temperature.[58] The situation may be further complicated by the presence of an intraligand $^3\pi\pi^*$ excited state that is energetically proximate to the ^{3}MLCT excited state, as observed for Re^I(s-phen)$(CO)_3$-Cl complexes (s-phen = 4,7-Me_2-1,10-phen, 5,6-Me_2-1,10-phen, 3,4,7,8-Me_2-1,10-phen).[59] The case of energetically proximate intraligand and charge-transfer excited states, however, does not appear to be pertinent to Re^I(phen)$(CO)_3$(phosphine)$^+$ complexes because the room temperature emission does not exhibit vibronic structure, which is a signature of $^3\pi\pi^*$ emission from transition-metal polypyridyl complexes.[60] Accordingly, we ascribe the emission band of Re^I(phen)$(CO)_3$(P-F)$^+$ shown in Figure 2 to a predominantly ^{3}MLCT parentage, as assigned for other Re(phen)$(CO)_3(L)^+$ (L ≠ phosphine) complexes with long lifetimes and similar emission envelopes.[61] As noted previously, removal of a CO ligand to form $Re^I(NN)(dicarbonyl)^+$ complexes lowers the energy of the ^{3}MLCT excited state relative to their tricarbonyl counterparts. In accordance with these observations, the emission band maximum of [Re(phen)(dppe)-$(CO)_2$](PF_6) is 2800 cm^{-1} to the red of [Re(phen)(P-F)$(CO)_3$]-(PF_6).

The precise determination of the ^{3}MLCT excited-state energy of the Re^I polypyridyl carbonyl complexes is problematic for several reasons. Location of the $E_{0,0}$ for the emitting state cannot be deduced from the overlap of the absorption and emission bands, as predicted by the Franck−Condon principle, because absorption occurs into the ^{1}MLCT state and emission occurs from the corresponding ^{3}MLCT state. Moreover, the room temperature emission bands of d^6 polypyridyl complexes are usually broad and featureless, and thus the $v' = 0 \rightarrow v = 0$ transition cannot be directly observed within the emission envelope. Evaluation of the emission energy from low-temperature glasses of Re^I complexes is further complicated by the rigidochromic effect.[41,62]

In the absence of a direct measure of the excited-state energy, a Franck−Condon analysis of the emission band shapes was employed. The values of E_0, S, frequency ($\hbar\omega$), and bandwidth ($\Delta\bar{\nu}_{1/2}$) listed in Table 2 were obtained by fitting the emission spectra shown in Figure 2 to eq 1. The E_0 and $\Delta\bar{\nu}_{1/2}$ values may be used calculate the free energy of the MLCT excited state, ΔG^o_{MLCT}, according to the following:[45,46]

$$\Delta G^o_{MLCT} = E_0 + \frac{(\Delta\bar{\nu}_{1/2})^2}{16\, k_B T \ln(2)} \qquad (3)$$

The values of ΔG^o_{MLCT} are listed in Table 2. Within the homologous polypyridyl series, Re(bpy)$(CO)_3$X, the decrease in ΔG^o_{MLCT} across the series X = CN^- > SCN^- > Cl^- is paralleled by a decrease in the emission quantum yields (Φ_{em}) and lifetimes (τ_{em}) listed in Table 1. This behavior is in accordance with the predictions of the energy gap law.[57]

Table 2. Emission Spectral Parameters Obtained from Fitting Corrected Emission Band to eq 1, and Energy of the MLCT Excited State Calculated from eq 3

compound	E_0 (cm^{-1})	S	$\hbar\omega$ (cm^{-1})	$\Delta\bar{\nu}_{1/2}$ (cm^{-1})	ΔG^o_{MLCT} (eV)
Re(bpy-COOH)$(CO)_3$Cl	16400	1.0	1900	2800	2.47
Re(bpy-COOH)$(CO)_3$SCN	16300	1.5	1700	3000	2.52
Re(bpy-COOHOH)$(CO)_3$CN	16800	0.8	2000	3100	2.60
Re(bpy-F)$(CO)_3$CN	16500	0.9	1800	3200	2.59
[Re(phen)(P-F)$(CO)_3$](PF_6)	20300	1.8	1200	1800	2.70
[Re(phen)(dppe)$(CO)_2$](PF_6)[a]	16700	0.7	1700	2600	2.42

[a] Solvent is CH_3CN.

There are several other notable features of the Φ_{em} and τ_{em} listed in Table 1. (1) [Re(phen)(dppe)$(CO)_2$](PF_6) in CH_3CN exhibits a slightly faster τ_{em} and lower Φ_{em} than that previously reported in the less polar CH_2Cl_2 solvent.[40] (2) Solutions of the benzyl amide conjugate, [Re(phen)(PP-Bn)$(CO)_2$](PF_6), exhibit biexponential emission decay behavior (τ_1 = 1.1 μs and τ_2 = 4.3 μs) as a result of a mixture of geometric isomers. A crystal of the isomer characterized by X-ray diffraction (shown in Figure 1) dissolved in CH_3CN exhibits a monoexponential decay (τ = 0.96 μs) equivalent to τ_1 of the isomer mixture. We, therefore, ascribe the short lifetime decay to the excited state of the isomer shown in Figure 1 and the longer lifetime decay to its isomeric congener. (3) The [Re(phen)$(CO)_3$(P-F)](PF_6) complex exhibits the longest τ_{em} and highest Φ_{em} and ΔG^o_{MLCT} of all the complexes in this study. The more energetic excited state and/or disposition of a phosphine trans to a CO may be responsible for a photolysis reaction that we observe for this complex upon extensive laser irradiation. A similar photochemical behavior observed for $Re^I(NN)(CO)_3(PR_3)^+$ complexes upon irradiation with light (λ > 320 nm) has been attributed to loss of a CO ligand.[56]

The high values of ΔG^o_{MLCT} for the amino acid conjugates, [Re(phen)$(CO)_3$(P-F)](PF_6) and Re(bpy-F)$(CO)_3$CN, make these platforms excellent candidates for promoting the oxidation of tyrosine directly from the excited state. The excited-state reduction potentials for the Re^I polypyridyl tricarbonyl complexes are listed in Table 3 along with the modified Latimer diagram from which they were determined. The portion of the diagram relevant to tyrosine oxidation is highlighted in black. The ground state $E°(Re^{I/0})$ and $E°(Re^{II/I})$ reduction potentials were determined from differential pulse voltammetry (DPV) measurements. Reversible electrochemical behavior is observed for the $E°(Re^{I/0})$ redox process, whereas the $E°(Re^{II/I})$ redox couple is quasi-irreversible and is, therefore, reported as a peak potential, E_p, in Table 3.

With the excited-state reduction potentials in hand, we next investigated the facility of tyrosine to quench the emission of these powerful excited-state oxidants. A comparison of the luminescence properties of Re(bpy-AA)$(CO)_3$CN (AA = Y and F) complexes in 10 mM aqueous phosphate buffer at pH 7 established no phosphorescence quenching of the tyrosine complex. However, deprotonation of the tyrosine phenol (pK_a = 10.1 for L-tyrosine)[63] at pH 12 induces significant emission

(57) Stufkens, D. J.; Vlèek, A., Jr. *Coord. Chem. Rev.* **1998**, *177*, 127.
(58) Striplin, D. R.; Crosby, G. A. *Chem. Phys. Lett.* **1994**, *426*, 426.
(59) Striplin, D. R.; Crosby, G. A. *Coord. Chem. Rev.* **2001**, *211*, 163.
(60) Ayala, N. P.; Flynn, C. M., Jr.; Sacksteder, L.; Demas, J. N.; DeGraff, B. A. *J. Am. Chem. Soc.* **1990**, *112*, 3837.
(61) Sacksteder, L.; Zipp, A. P.; Brown, E. A.; Streich, J.; Demas, J. N.; DeGraff, B. A. *Inorg. Chem.* **1990**, *29*, 4335.
(62) Lumpkin, R. S.; Meyer, T. J. *J. Phys. Chem.* **1986**, *90*, 5307.
(63) Tommos, C.; Skalicky, J. J.; Pilloud, D. L.; Wand, S. J.; Dutton, P. L. *Biochemistry* **1999**, *38*, 9495.

Table 3. Differential Pulse Voltammetry[a] and Excited-State Reduction[b] and Oxidation Potentials[c] of Amino Acid-Derivatized Re^{I} Polypyridyl Tricarbonyl Complexes

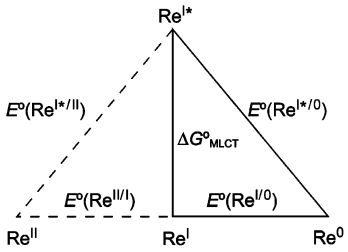

complexes	E_p ($Re^{II/I}$)[a]	$E°$ ($Re^{I/0}$)[a]	$E°$ ($Re^{I*/0}$)[b]	$E°$ ($Re^{I*/II}$)[c]
Re(bpy-A-O*t*Bu)$(CO)_3$Cl	0.94	−1.58		
Re(bpy-F)$(CO)_3$CN	1.09	−1.65	1.59	0.85
[Re(phen)(P-F)$(CO)_3$](PF_6)	1.52	−1.57	1.78	0.53

[a] Reported in volts vs Fc^+/Fc with 0.1 M $(Bu_4N)PF_6$ as supporting electrolyte in CH_3CN. [b] $E°(Re^{I*/0}) = \Delta G°_{MLCT} + E°(Re^{I/0})$ vs NHE. [c] $E°(Re^{I*/II}) = \Delta G°_{MLCT} - E°(Re^{II/I})$ vs NHE.

quenching. A rate constant for this process may be determined from the excited-state lifetimes in the presence and absence of quenching

$$k_q = \frac{1}{\tau_Y} - \frac{1}{\tau_F} \qquad (4)$$

where τ_Y and τ_F are the lifetimes of emission decay for the Y and F derivatives, respectively. The measured lifetime of τ_Y = 1.2 ns for Re(bpy-Y)$(CO)_3$CN yields a $k_q = 8.2 \times 10^8\ s^{-1}$.

In contrast to the pH behavior of Re(bpy-Y)$(CO)_3$CN quenching, the emission from [Re(phen)(P-Y)$(CO)_3$](PF_6) was quenched at all pHs. At pH 7, $\tau_Y = 2.2\ \mu s$ and $\Phi_{em,Y} = 0.059$ for the tyrosine derivative whereas $\tau_F = 3.9\ \mu s$ and $\Phi_{em,F} = 0.094$ for the phenylalanine derivative (τ_F and $\Phi_{em,F}$ are independent of pH), yielding a quenching rate constant of $k_q = 2.0 \times 10^5\ s^{-1}$. As noted above, the [Re(phen)(P-AA)$(CO)_3$](PF_6) complexes are subject to CO dissociation under prolonged irradiation. We contend that the kinetics for CO dissociation upon complex excitation are the same for the F and Y derivatives and do not vary with pH. Under this assumption, eq 4 isolates the quenching process due to Y. k_q for [Re(phen)(P-Y)$(CO)_3$]-(PF_6) exhibits the pH dependence shown in Figure 3 as a result of the pH dependent τ_Y. The points are separated into three color-coded regions to represent the different protonation states of the tyrosine residue; black and red points correspond to the protonated and deprotonated forms of the tyrosine carboxylic acid, respectively, while the green points are for the deprotonated tyrosine phenol. Above pH 10, the quenching of the excited state increases significantly; the vestige of this increase is indicated by the displaced rate constant at pH 10. The quenching mechanism appears to change at basic pHs due to the aforementioned lability of the sixth coordination site of $Re(CO)_3(NN)^+$. We believe that phosphine is substituted upon intramolecular attack of the phenolate oxygen of the deprotonated tyrosine. We rule out an intermolecular attack by hydroxide as the excited-state lifetime of [Re(phen)(P-F)$(CO)_3$](PF_6) does not change at very basic pHs.

Nanosecond transient absorption spectroscopy establishes that the quenching process of the tyrosine derivatives occurs by charge transfer. The transient absorption profiles following 355 nm excitation of the Re(bpy-Y)$(CO)_3$(CN) complex in pH 7 and 12 solutions are presented in Figure 4. The ΔOD spectrum at pH 7 is the same as that obtained for Re(bpy-F)$(CO)_3$(CN) at all pHs (not shown) and consists of maxima at 380 and ~475 nm and a minimum at 400 nm. These features are in accord with that observed for the ^{3}MLCT state of $Re^{I}(NN)(CO)_3L$ complexes.[57,64] In support of a similar assignment here, the single wavelength transient signals obtained at 380 and 475 nm shown in the top insets of Figure 4 decay to baseline with time constants (61 and 60 ns, respectively) identical to the emission lifetime of the ^{3}MLCT excited state (60 ns). In contrast, time-resolved absorption spectra of Re(bpy-Y)$(CO)_3$(CN) at pH 12 are not that of the ^{3}MLCT excited state. The transient profile is dominated by absorptions at 410 and 520 nm. The 410 nm feature coincides with the absorption maximum of $Y^{\bullet}$,[65] and the 520 nm feature resembles the absorption maxima of $bpy^{\bullet-}$.[66,67] With regard to the latter, the TA feature is similar to the spectroelectrochemical UV−vis absorption spectrum of the reduced Re($bpy^{\bullet-}$-Y-O*t*Bu)$(CO)_3$CN in DMF (shown in Figure S3 in the Supporting Information). These results provide direct evidence for the charge separated state, Re($bpy^{\bullet-}$-$Y^{\bullet}$)$(CO)_3$(CN). The time-evolved gray traces establish that the overall profile does not change with time. The single wavelength transient signals obtained at 410 and 500 nm and shown in the bottom insets decay concomitantly with a rate constant of $k_{CR} = 2.2 \times 10^7\ s^{-1}$, which we attribute to charge recombination. The low solubility of [Re(phen)(P-Y)$(CO)_3$](PF_6) in water prevented its investigation by transient absorption methods.

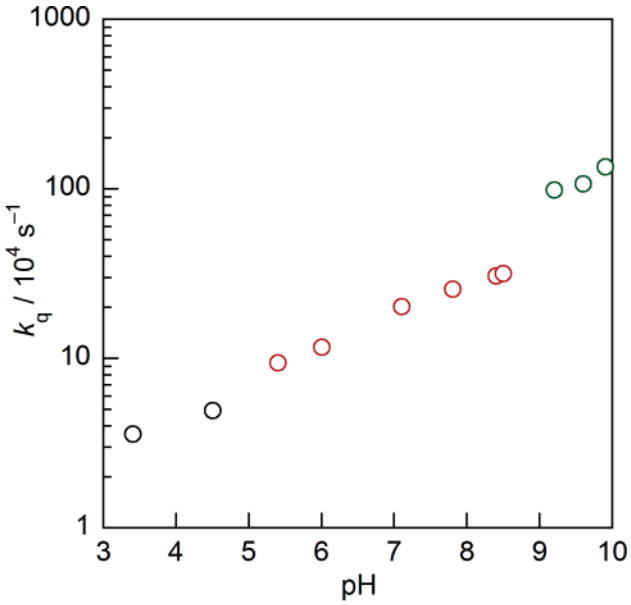

Figure 3. Plot of the rate constant for emission quenching, k_q, versus pH for [Re(P-Y)(phen)$(CO)_3$]PF_6. Three pH regions are highlighted corresponding to the protonated (black circles) and deprotonated (red circles) forms of the tyrosine carboxylic acid and deprotonated (green circles) tyrosine phenol.

Discussion

Rhenium(I) polypyridyl complexes provide suitable platforms for the intramolecular photogeneration of tyrosyl radicals, owing

(64) Kalyanasundaram, K.; Graetzel, M.; Nazeeruddin, M. K. *Inorg. Chem.* **1992**, *31*, 5243.
(65) Bent, D. V.; Hayon, E. *J. Am. Chem. Soc.* **1975**, *97*, 2599.
(66) Damrauer, N. H.; McCusker, J. K. *J. Phys. Chem. A* **1999**, *103*, 8440.
(67) Krejèík, M.; Vlèek, A. A. *J. Electroanal. Chem.* **1991**, *313*, 243.

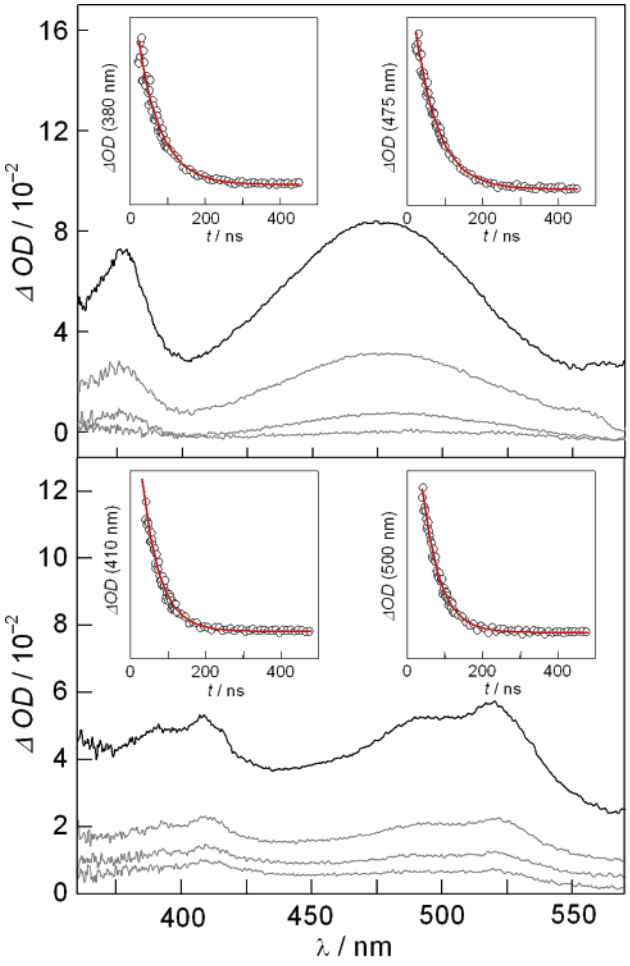

Figure 4. Top: Transient absorption spectra following 355 nm laser excitation (fwhm = 3 ns) of pH 7 solution of Re(bpy-Y)$(CO)_3$(CN) at 15 (black line) and 65, 115, and 215 ns (gray line, top to bottom). Insets: Single wavelength kinetic traces and monoexponential fits for the disappearance of the 380 and 475 nm (^{3}MLCT) signals. Bottom: Same experiment at pH 12 over the same time course of the top panel. Insets: Single wavelength kinetic traces and monoexponential fits for the disappearance of the 410 ($Y^\bullet$) and 500 nm ($bpy^{\bullet-}$) signals.

to the significant oxidizing power of their MLCT excited states. The driving force for the intramolecular MLCT quenching process, ΔG°_{PCET}, is

$$\Delta G^\circ_{PCET} = E^\circ(Re^I*/0) - E^\circ(Y^\bullet/Y) \qquad (5)$$

where $E^\circ(Re^I*/0)$ is given in Table 3, and $E^\circ(Y^\bullet/Y)$ is the previously reported pH-dependent reduction potential for $Y^\bullet$.[63] In the above expression, ΔG°_{PCET} is not corrected for Debye−Huckel electrostatic work terms since the $Y^\bullet$ radical is neutral. The Re^I complexes have considerable overpotential for the oxidation of tyrosine, but two observed results suggest that $Y^\bullet$ generation does not proceed by a simple ET. (1) Despite significant oxidizing strength at all pHs, the MLCT excited state of Re(bpy-Y)$(CO)_3$CN is only a competent oxidant of tyrosine when it is deprotonated (pH > 10). (2) Although [Re(P-Y)-(phen)$(CO)_3$]PF_6 oxidizes Y at all pHs, Figure 3 shows that the rate constant for this process is pH-dependent. Taken together, these results clearly indicate a pronounced role for the proton in $Y^\bullet$ generation and implicate proton-coupled electron transfer (PCET) as the mechanism for tyrosine oxidation.

The energetics of the PCET contribution to $Y^\bullet$ generation is accounted for by the pH dependence of $E^\circ(Y^\bullet/Y)$[63]

$$E^o(Y^\bullet/Y) = E^o(Y^\bullet/Y^-) + \frac{2.303RT}{nF}\log\left(1 + \frac{10^{-pH}}{10^{-pK_a(Y)}}\right) \qquad (6)$$

where $E^\circ(Y^\bullet/Y^-)$ is the reduction potential for forming the deprotonated tyrosine phenolate (0.65 V vs NHE), and $pK_a(Y)$ is that for the tyrosine phenol (9.9 for *N*-acetyl-L-tyrosinamide).[63] The overall form of the pH-dependent quenching, shown in Figure 3, is in accordance with the predictions of eq 6. At low pH, tyrosine is more difficult to oxidize, and rates for $Y^\bullet$ generation should be slowest. A smoothly varying monotonic increase in the rate constant is expected as the pH is increased to the pK_a of the tyrosine. This overall behavior is generally observed excepting a discontinuity at pH ∼ 5, as indicated by the different color coding in Figure 3. At this pH, the carboxylic acid group of the amino acid backbone is deprotonated, augmenting the dipole moment of the ground-state complex in a direction favorable for ET.[27,68,69] The slight displacement of the quenching rate constants and increase in slope in the pH = 5−9 range are consistent with this behavior. After pH = $pK_a(Y)$, the rate constant should be invariant to pH changes as is $E^\circ(Y^\bullet/Y^-)$ for the deprotonated tyrosine phenolate. The green points represent the ET rate for oxidation of the deprotonated tyrosine phenolate without interference of the proton. A similar jump in the rate constant of tyrosine oxidation upon its deprotonation has been observed by Sjödin et al.,[34] who used a flash-quench-generated Ru^{III} oxidant to photogenerate tyrosyl radical appended to a bpy ligand.

The inability to oxidize Y with the shorter-lived MLCT excited state of the Re(bpy-Y)$(CO)_3$(CN) complex is also consistent with a PCET mechanism. The PCET rate constant for intramolecular quenching of [Re(phen)$(CO)_3$(P-Y)]PF_6 (at pH < 9) is an order of magnitude slower than the ET rate constant for [Re(phen)$(CO)_3$(P-Y^-)]PF_6 oxidation (at pH > 9). A similar order of magnitude decrease in the rate of $Y^\bullet$ formation for Re(bpy-Y)$(CO)_3$(CN) would furnish a PCET rate of 10^6 s^{-1}, which barely competes with the normal excited-state decay (10^7 s^{-1}). Thus, our inability to observe excited-state quenching for this complex at pHs where Y is protonated is reasonable. Conversely, the higher driving force for Y oxidation in [Re(phen)$(CO)_3$(P-Y)]PF_6, coupled to its longer-lived ^{3}MLCT excited state, allows for the relatively sluggish PCET reaction (k_{PCET} = 1.6 × 10^5 s^{-1} at pH 7) to be observed.

Intramolecular shuttling of electrons between tyrosine and the MLCT excited state may occur along two fundamentally different pathways, designated in Scheme 2 as pop−pop and pop−fizz. The latter describes the electron-transfer events induced by excitation of typical Re(NN)$(CO)_3$X complexes, in which the donor is attached to the polypyridyl ligand, as is the case for Re(bpy-Y)$(CO)_3$CN. Photon absorption ("pop") forms the ^{3}[Re^{II}($bpy^{\bullet-}$-Y)$(CO)_3$CN] MLCT state. Subsequent tyrosine oxidation occurs by a contraposed electron flow, whether through the bpy or through space. The pathway is anticipated to incur several barriers to $Y^\bullet$ generation. Oxidation of tyrosine brings the electron through the reduced bpy ligand. Though the effect of superexchange through a reduced polypyridyl ligand

(68) Batchelder, T. L.; Fox, R. J., III; Meier, M. S.; Fox, M. A. *J. Org. Chem.* **1996**, *61*, 4206.
(69) Galoppini, E.; Fox, M. A. *J. Am. Chem. Soc.* **1996**, *118*, 2299.

Scheme 2

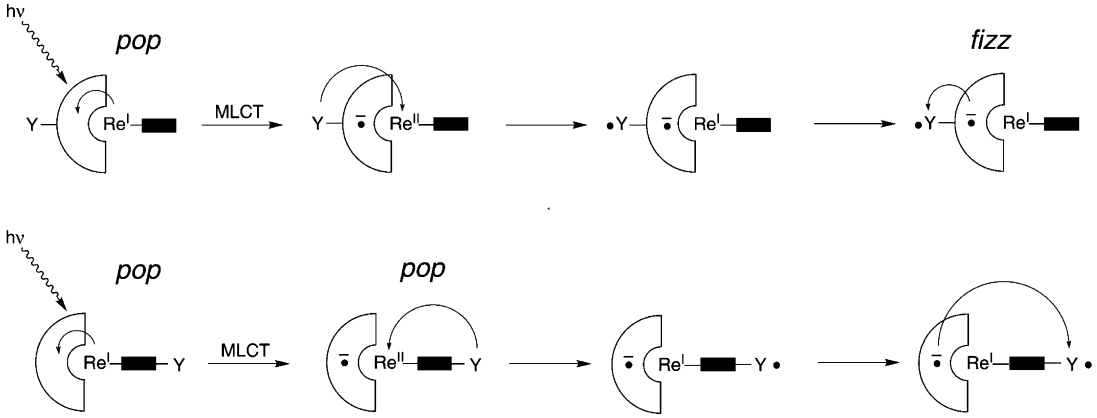

has not been investigated critically, general theory suggests that the increased energy gap between reduced donor and oxidized acceptor levels would retard the tunneling rate for Y• generation.[70] More problematic is the favored back reaction resulting from the disposition of a neighboring hole and electron on Y• and bpy•−, respectively. The correlation between the back electron-transfer rate and proximity of hole/electron pairs has been examined in a comparative study of $Re^{I}(bpy)(CO)_3(py)^+$ complexes containing a phenothiazine (PTZ) electron donor coupled to the pyridine ligand in $Re(4,4'\text{-}Me_2\text{-}bpy)(CO)_3(py\text{-}PTZ)^+$ and bipyridine ligand in $Re(PTZ\text{-}CH_2\text{-}bpy)(CO)_3(4\text{-}Etpy)^+$.[71] An accelerated back electron-transfer rate was established for the former, which exhibits a $Re(PTZ^{\bullet+}\text{-}CH_2\text{-}bpy^{\bullet-})(CO)_3(4\text{-}Etpy)^+$ charge distribution upon intramolecular quenching of the MLCT excited state. A similar charge distribution is retained in the charge-separated state of the tyrosine-modified Re^{I} polypyridyl complex, $Re^{I}(bpy^{\bullet-}\text{-}Y^{\bullet})(CO)_3\text{-}CN$, thus accounting for its short lifetime of 45 ns ("fizz").

The hole/electron pair is optimally separated by appending the tyrosine ligand to the sixth ligand, away from the polypyridyl ligand. We chose phosphine ligands as the scaffold for the amino acid owing to the high energies and long lifetimes of $Re(NN)(PP)(CO)_2^+$ and $Re(NN)(P)(CO)_3^+$ model compounds. Of these two platforms, the latter was more ideally suited to Y• generation owing to a greater water solubility and intrinsically higher MLCT excited-state energy. The architecture of the $Re^{I}(phen)(CO)_3(P\text{-}Y)^+$ complex permits the charge distribution in the pop−pop pathway of Scheme 2 to be established. Excitation pops the electron to the phen ligand in the MLCT state to produce $Re^{II}(phen^{\bullet-})(CO)_3(P\text{-}Y)^+$, which then allows for the electron to flow from the phosphine ligand, quenching the Re^{II} hole, and furnishing the $Re^{I}(phen^{\bullet-})(CO)_3(P\text{-}Y^{\bullet})^+$ radical intermediate. The electron and hole are disposed at maximal distance within the primary coordination sphere of the complex, presumably retarding the rate of charge recombination.

Conclusions

Phosphines of Re^{I} polypyridyl complexes are ideal platforms for the direct intramolecular photogeneration of amino acid radicals, and especially tyrosine for three reasons. First, the MLCT excited state is highly energetic and presents a significant overpotential for tyrosine oxidation. The additional energy of the MLCT excited state is crucial for amino acid oxidation because, unlike a simple ET quenching process, it is needed to overcome the barrier for proton transfer, as well.[34,72] Second, the phosphine complexes exhibit a dramatically extended lifetime of the MLCT excited state, allowing for a higher Stern−Volmer constant ($SV = k_q\tau_o$) for quenching.[73] Finally, by appending the tyrosine to an ancillary ligand, remote from the electron-accepting polypyridyl ligand in MLCT excitation, the intramolecular shuttling occurs via a unidirectional electron cascade for the efficient generation and preservation of the photogenerated Y•.

The Re^{I} phosphine scaffolds presented here provide a convenient method for investigating radical-based mechanisms in biology because, unlike previous approaches, the amino acid radical can be generated directly and on microsecond time scales without the need for external oxidants or reductants. Moreover, unlike previous Re^{I} complexes used to photogenerate tyrosyl radicals, such as $Re^{I}(phen)(CO)_3(His)^+$, the Re^{I} phosphine complexes are resistant to carboxylate exchange. Thus, these MLCT states may be used to initiate and study radical reactions on peptides or within proteins containing multiple aspartate or glutamate residues. Finally, we note that this method is not necessarily specific to tyrosine but can be extended to other amino acids by simple derivatization of the monophosphine.

The complexes reported here are particularly convenient for phototriggering amino acid radicals in biological PCET pathways because the kinetics are not convoluted with the bimolecular events of the flash-quench process. The simplicity of this approach is especially beneficial for the study of the PCET pathway in class I RNR, which catalyzes the conversion of nucleotides to deoxynucleotides, providing all of the monomeric precursors required for DNA replication and repair in the host organism.[74] Enzyme function is derived by connecting a radical initiation site (•Y122, *E. coli* numbering) to a cysteine (C439) at the active site of substrate turnover through a 35 Å radical transport pathway that spans two subunits (R2 and R1).[75] This intersubunit pathway is postulated to be gated by a tyrosine, Y356,[22−25] which is located near the C-terminus of R2 and is the bellwether of a YYY pathway, Y356 → Y731 → Y730 →

(70) Lewis, F. D.; Liu, J.; Weigel, W.; Rettig, W.; Kurnikov, I. V.; Beratan, D. N. *Proc. Natl. Acad. Sci. U.S.A.* **2002**, *99*, 12536.
(71) Chen, P.; Duesing, R.; Graff, D. K.; Meyer, T. J. *J. Phys. Chem.* **1991**, *95*, 5850.
(72) Sjödin, M.; Ghanem, R.; Polivka, T.; Pan, J.; Styring, S.; Sun, L.; Sundström, V.; Hammarström, L. *Phys. Chem. Chem. Phys.* **2004**, *6*, 4851.
(73) Balzani, V.; Moggi, L.; Manfrin, M. F.; Bolletta, F. *Coord. Chem. Rev.* 1975, *15*, 321.
(74) Jordan, A.; Reichard, P. *Annu*. Rev. Biochem. **1998**, *67*, 71.
(75) Uhlin, U.; Eklund, H. *Nature* **1994**, *370*, 533.

C439. Radical transport along this pathway may be examined by synthesizing modified variants of the 20-mer C-terminal peptide tail of the R2 subunit. This peptide segment preserves the binding determinant of R2 to R1, and it contains the critical Y356, as well. The inclusion of phototriggers proximate to Y356 in the heavily carboxylated C-terminus tail provides a method for generating Y356$^{\bullet}$ without the need for R2.[15] In this way, radical transport along the Y356 → Y731 → Y730 → C439 pathway can be "turned on" promptly by laser excitation of the 20-mer peptide terminus of R2 bound to R1. Moreover, Y356$^{\bullet}$ may be photogenerated with excitation wavelengths that lie well outside the protein absorption envelope ($\epsilon_{280} = 190\,000$ M^{-1} cm^{-1}), and the relatively fast time scale ($>10^6$ s^{-1}) for Y generation provides a large temporal window through which to observe Y356 → Y731 → Y730 → C439 radical transport. Experiments to couple $Re^{I}(phen)(CO)_3(P\text{-}Y)^+$ to the C-terminal R2 19-mer peptide are currently underway.

Acknowledgment. We thank Linda M. Rodriguez for insights into electron shuttling mechanisms and nomenclature, Michelle C. Y. Chang and Jeffrey Hirsch for preliminary contributions to the synthesis of $Re(bpy\text{-}AA)(CO)_3^+$ complexes, David R. Manke for assistance with crystallography, and Durwin R. Striplin for contributions to our understanding of Re^{I} photophysics. We thank the National Institutes of Health for support of this work, GM47274.

Supporting Information Available: Crystal structure of $[Re(phen)(dppe)(CO)_2](PF_6)$; atom numbering schemes, tables of crystal data, atomic coordinates, bond lengths and angles, anisotropic thermal parameters, and hydrogen coordinates for $[Re(phen)(PP\text{-}Bn)(CO)_2](PF_6)\cdot CDCl_3$ and $[Re(phen)(dppe)(CO)_2](PF_6)$; X-ray crystallographic files, in CIF format; spectroelectrochemical spectrum for reduction of Re(bpy-Y-O*t*Bu)$(CO)_3CN$. This material is available free of charge via the Internet at http://pubs.acs.org.

JA0510360